ACS SyntheticBiology

Research Article

pubs.acs.org/synthbio

Resource Sharing Controls Gene Expression Bursting

Patrick M. Caveney,[†,‡] S. Elizabeth Norred,[†,‡] Charles W. Chin,[†,‡] Jonathan B. Boreyko,[†,‡,§] Brandon S. Razooky,[‡,∥] Scott T. Retterer,[†,‡,⊥] C. Patrick Collier,[‡] and Michael L. Simpson*[,†,‡,#]

[†]Bredesen Center, University of Tennessee, Knoxville, Tennessee 37996-2010, United States

[‡]Center for Nanophase Materials Sciences, Oak Ridge National Laboratory, Bethel Valley Road, Oak Ridge, Tennessee 37831, United States

[§]Department of Biomedical Engineering and Mechanics, Virginia Tech, Blacksburg, Virginia 24061, United States

[∥]Laboratory of Immune Cell Epigenetics and Signaling, The Rockefeller University, New York, New York 10065, United States

[⊥]Biosciences Division, Oak Ridge National Laboratory, Oak Ridge, Tennessee 37831, United States

[#]Joint Institute for Biological Sciences, University of Tennessee–Knoxville and Oak Ridge National Laboratory, Bethel Valley Road, Oak Ridge, Tennessee 37831, United States

S *Supporting Information*

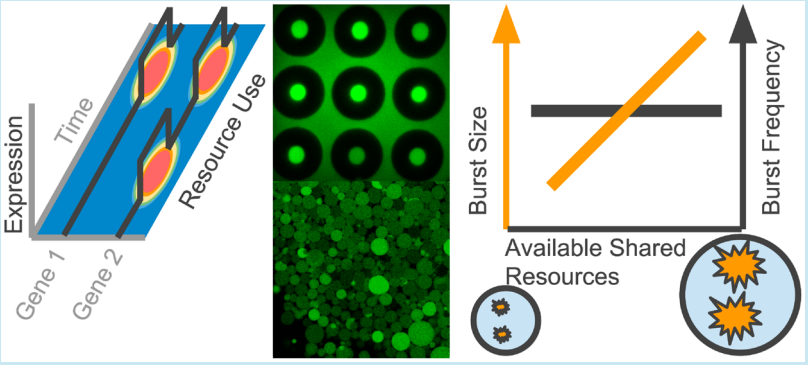

ABSTRACT: Episodic gene expression, with periods of high expression separated by periods of no expression, is a pervasive biological phenomenon. This bursty pattern of expression draws from a finite reservoir of expression machinery in a highly time variant way, i.e., requiring no resources most of the time but drawing heavily on them during short intense bursts, that intimately links expression bursting and resource sharing. Yet, most recent investigations have focused on specific molecular mechanisms intrinsic to the bursty behavior of individual genes, while little is known about the interplay between resource sharing and global expression bursting behavior. Here, we confine *Escherichia coli* cell extract in both cell-sized microfluidic chambers and lipid-based vesicles to explore how resource sharing influences expression bursting. Interestingly, expression burst size, but not burst frequency, is highly sensitive to the size of the shared transcription and translation resource pools. The intriguing implication of these results is that expression bursts are more readily amplified than initiated, suggesting that burst formation occurs through positive feedback or cooperativity. When extrapolated to prokaryotic cells, these results suggest that large translational bursts may be correlated with large transcriptional bursts. This correlation is supported by recently reported transcription and translation bursting studies in *E. coli*. The results reported here demonstrate a strong intimate link between global expression burst patterns and resource sharing, and they suggest that bursting plays an important role in optimizing the use of limited, shared expression resources.

KEYWORDS: *gene expression, bursting, confinement, resource sharing, cell-free, microfluidics*

Bursty or episodic gene expression—periods of high expression separated by periods of very low or no expression—is a widespread phenomenon observed across biological domains.[1−7] The common gene expression burst pattern (Figure 1a) consists of short intense periods of expression separated by relatively long periods without expression.[6,8,9] This bursty pattern of expression draws from a finite reservoir of reusable expression machinery, e.g., polymerases and ribosomes, in a highly time variant way. Thus, the majority of expressed genes require no resources most of the time, yet these genes draw heavily on them during short intense bursts. The reservoir of expression machinery is common to all genes in the organism, and many studies have addressed how, in a time-averaged way, expression resources are shared among genes.[10−12] Thus, genes with no direct regulatory relationships still interact through expression resource sharing.[11,13−15] However, little is understood about the relationships (if any)

Received: July 7, 2016

DOI: 10.1021/acssynbio.6b00189
ACS Synth. Biol. XXXX, XXX, XXX−XXX

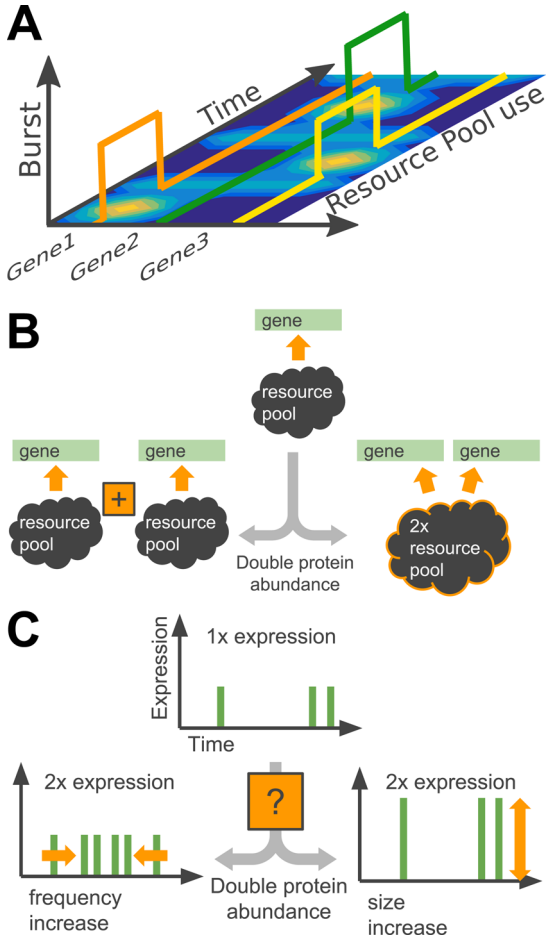

Figure 1. Bursty gene expression impact on global resource utilization. (a) Bursty gene expression draws heavily from shared global resource pools but only for limited durations. (b) Increasing protein abundance by increasing the number of genes and the amount of expression resources. The larger resource pool may be shared by all of the genes (right), or the sharing of resources may be enforced by compartmentalization (left). (c) Protein abundance changes may be driven by an increased expression burst size (right) or bust frequency (left). Does the resource sharing scenario affect the expression burst pattern?

that exist between expression bursting patterns and resource sharing.

Gene expression bursting studies have most often focused on molecular processes that are not directly related to resource sharing. Translational bursting, occurring when many proteins are synthesized from reading the same mRNA molecule, is initiated by the birth of an mRNA molecule and terminated by its decay. Transcriptional bursting has been shown, at least in part, to be controlled by molecular processes such as transcription factor kinetics,[16−18] promoter architecture,[19−22] chromatin remodeling,[21,23] supercoiling,[24] and transcriptional reinitiation.[3,25,26] Such a view sees expression bursting primarily as an intrinsic property of individual gene circuits. However, given the demands that an expression burst places on the common cellular pool of resources, this intrinsic view of bursting may be overly limiting. Instead, it seems likely that changes in the size of the common reservoir of expression machinery or in the number of genes drawing upon these resources (Figure 1b) will globally impact expression burst patterns (Figure 1c).

Studies of gene expression patterns have been carried out using various experimental techniques[6,19,27−30] in cells or in cell-free systems that were not confined to cellular-scale reaction chambers. Cell-based platforms provide the important advantage of viewing function within its natural context, but it is difficult to manipulate specific parameters, such as confinement, when they are isolated from all the other cellular processes, such as growth, cell division, and global gene expression.

Conversely, *in vitro* reaction chambers are especially suited for isolating the effects of specific mechanisms from confounding cellular processes,[31−35] and cell-free protein synthesis (CFPS) systems have been successfully used to observe gene expression bursting.[24] Recently, arrays of microfabricated cellular-scale reaction chambers have been demonstrated to be a viable way to confine CFPS reactions to study gene expression, in particular the noise in expression.[36,37] Bursting and noise are inseparably linked as bursting is often the dominant contributor to expression noise,[6,8,26,29,38] and noise measurements are often used to understand the underlying dynamics of gene expression *in vivo*.[6,8,39,40] In combination, microfabricated cell-scale reactors and gene expression noise measurements provide a unique platform to explore gene expression bursting and resource sharing in well-controlled and easily manipulated environments.

Here, we study cell-free gene expression in synthetic reaction chambers under different resource sharing scenarios. Specifically, we measure gene expression burst patterns as the number of genes and size of the resource pool are increased (i.e., the volume of the reaction chamber is increased) either by summing together discrete individual chambers (discrete resources; Figure 1b, left) or by making one larger chamber (shared resources; Figure 1b, right). As expected for both cases, total protein production and production rate scaled linearly with the amount of DNA and expression resources. However, while the discrete resources case (i.e., summed smaller chambers) generated higher protein abundance through more frequent bursts (Figure 1c, left), the shared resource case (i.e., individual larger chambers) drove increased protein production by increased burst sizes (Figure 1c, right). Surprisingly the divergent bursting behavior was found even though a constant ratio between expression resources and DNA was maintained for both scenarios, showing that resource sharing and expression bursts are directly coupled. For transient expression in cell-free expression chambers, we present a model that suggests this behavior emerges from the timing of mRNA production and size of the available resource pool. The mRNA molecules produced early consume most of the translational resources and make many proteins, whereas mRNAs produced later are created in a resource poor environment and make few proteins. As a result, in all cases the same number of mRNA molecules is responsible for the majority of protein production, but in the large chambers, those few mRNA molecules experience a very large translational burst size. This model of self-reinforcement of bursts may explain the robust positive correlation observed between transcriptional and translational burst sizes in *Escherichia coli*[41] and suggests that burst size control is the principle mechanism driving protein abundance changes.

RESULTS

To confine cell-free expression reactions, we fabricated actuatable polydimethylsiloxane (PDMS) cylindrical chambers on membranes suspended above microfluidic channels using soft lithography as described earlier.[37] All chambers were 5 μm deep but ranged in diameter from 2 to 10 μm and in volume from ∼15 to ∼400 fL, respectively. A 25 μL commercial raw

DOI: 10.1021/acssynbio.6b00189
ACS Synth. Biol. XXXX, XXX, XXX−XXX

extract CFPS reaction was mixed with 500 ng of enhanced green fluorescent protein (EGFP)-coding pET3a plasmid and was confined within the chambers through a two-step process described previously.[37] First, the cell-free mixture was loaded into the microfluidic channel using <10 psi of pressurized nitrogen, and then the membrane was actuated with ~20 psi of DI water to seal the reaction chambers (Figure 2a). Since the chambers were actuated and imaging began very soon, ~4 min, after plasmids were added to the CFPS mixture, this experimental platform provided a well-defined t = 0, i.e., the time when expression began, thereby allowing for the direct comparison of results from experiments performed on different days (Supporting Information Figure 1). Additionally, through microfabrication techniques, the reaction chamber size could be easily and accurately defined.

The time course of protein expression was characterized by measuring total fluorescence of EGFP within individual chambers every 3 min for 1 h (Figure 2b; Methods). Time courses averaged across all 119 individual chambers were similar to those observed in bulk reactions, although as reported elsewhere[42,43] confined reactions did proceed at a slightly increased rate (Supporting Information Figure 2). The fluorescence transients exhibited a relatively rapid increase in protein expression initially, followed by a much slower rate of GFP accumulation. This two-phase expression profile is consistent with resource limitations and not equilibrium between protein decay (e.g., photobleaching; Supporting Information Figures 3 and 4) and synthesis.[36,44] Similar to cellular experiments,[45] there was considerable chamber-to-chamber variation in the final fluorescence levels, yet there was a striking uniformity to the shape of the transient response between experiments and chamber sizes (Supporting Information Figures 1 and 5).

This uniformity in transient response allowed the use of a previously described method[6,36,46] to extract the noise from each individual trace (Figure 2d; Methods). Briefly, the deterministic transient response was removed from each trace. The remaining signals were assumed to be due only to the stochastic fluctuations in the gene expression process, i.e., the expression noise. The magnitude of the expression noise within an individual chamber was quantified using the square of the coefficient of variation (CV^2; variance/[final fluorescent abundance]^2). The CV^2 of individual chambers and the composite CV^2 of all chambers of the same size were plotted versus their final fluorescence abundance (Figure 2d). Similar to cellular experiments,[6,45] the CV^2 values of individual chambers were scattered around the composite CV^2 oriented along a line inversely proportional to final fluorescence intensity.

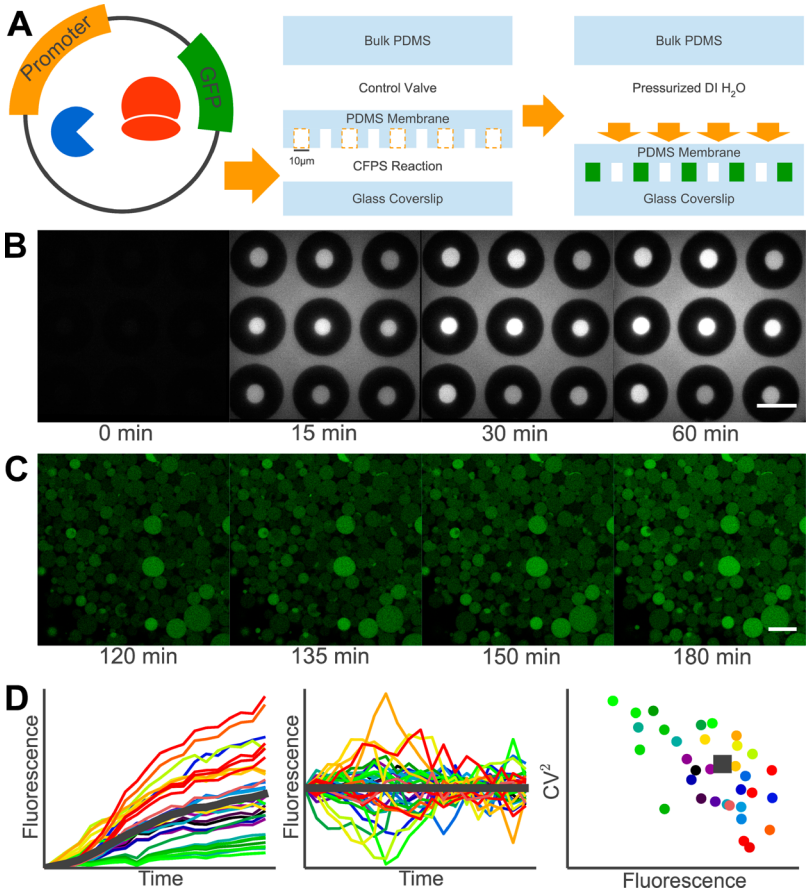

Figure 2. Confined cell-free gene expression and noise measurements. (a) Cell-free protein synthesis (CFPS) reactions expressing EGFP were isolated within microfabricated chambers. (b) Time-lapse fluorescence microscopy was used to image the confined reactions every 3 min for 1 h. Images from an expression experiment performed in 10 μm diameter reaction chambers show fluorescence intensity increasing over time. Scale bar, 20 μm. (c) Representative z-slice of POPC vesicles expressing EGFP. Imaged every 3 min for 1 h. Scale bar, 20 μm. (d) (left) Time history of the growth of the protein population collected for each chamber. (middle) Gene expression noise found by removing the deterministic general trend from each expression transient. (right) CV^2 and final fluorescence level (protein abundance) for individual chambers (colored circles) and for the average of all chambers (gray square).

DOI: 10.1021/acssynbio.6b00189
ACS Synth. Biol. XXXX, XXX, XXX−XXX

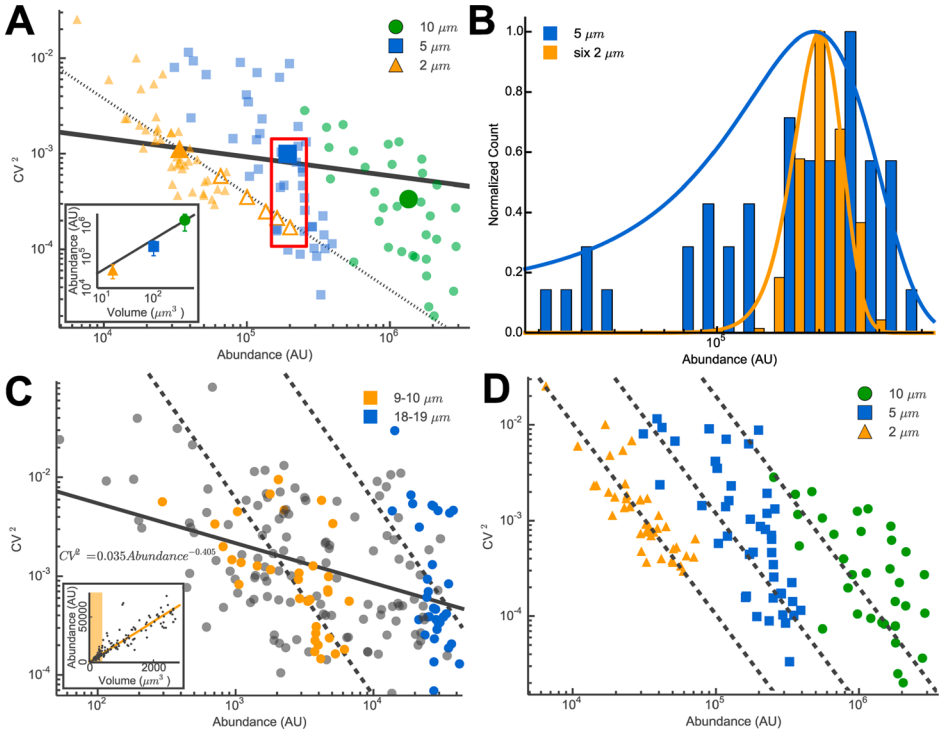

Figure 3. Effects of resource pool size and configuration on gene expression noise in both microfluidic chambers and vesicles. (a) CV^2 vs protein abundance for 2, 5, and 10 μm diameter chambers. The small filled data points represent individual chambers, and the large filled data points show the mean behaviors for all chambers of a given size. The dotted line is of the form a/abundance, and where a is a constant that is calibrated so the line passes through the mean of the 2 μm diameter chambers (large filled orange triangle). The open orange triangles show combinations of 2 μm chambers. The left most open triangle shows the average behavior of sums of two individual 2 μm chambers, and the right most open triangle shows the average behavior of sums of six individual 2 μm chambers. CV^2 for these combinations of 2 μm chambers closely follow the a/abundance trend. In contrast, the individual 5 μm chambers deviate strongly (solid line) from the a/abundance trend even though their volume and protein abundance are about equal to six 2 μm chambers (red box). The inset shows that protein abundance scales approximately linearly with volume. (b) Histograms of protein abundance across the ensemble of individual 5 μm chambers (blue) and the ensemble of combinations of six 2 μm chambers (orange). Histograms are normalized (i.e., frequency of most likely protein abundance is set to 1) and fit with normal distributions (solid lines). (c) CV^2 vs protein abundance for vesicles ranging in diameter from 4 to 19 μm. Each data point (gray or colored) represents an individual vesicle. The orange points are vesicles with diameters of 9−10 μm, and the blue points have diameters of 18−19 μm. The solid line is a power law fit to all points. While abundance varies by 3 orders of magnitude, CV^2 values decrease only by about 1 order of magnitude. Dashed lines show fits to individual volumes (orange and blue), where CV^2 goes as 1/abundance^2. The inset shows that protein abundance scales linearly with vesicle volume. The shaded region on the inset corresponds to the volume range explored using the chambers. (d) Same data in (a) without means. Dashed lines are fits to each size chamber where CV^2 goes as 1/abundance^2.

The baseline expression noise vs abundance relationship (Figure 3a) of this experimental system was established using the average behavior of the 2 μm chambers (large filled orange triangle). To study the effects of resource sharing on gene expression noise and bursting, the volume of the reaction was increased from this baseline in two ways. First, composite chambers were created by summing fluorescence signals from between two and six individual 2 μm chambers (open orange triangles Figure 3a). These composite chambers allowed for the total reaction volume to be varied while ensuring that expression resources were shared exactly as they were in the individual 2 μm chambers. Average final fluorescence levels in these composite chambers scaled linearly with volume, and as expected,[4,6,30,47] CV^2 scaled linearly with the inverse of abundance (Figure 3a dotted line). This behavior indicated that expression within each of the chambers was similar to, but statistically independent of, the other chambers included in the sum. Said differently, the number of expression bursts, or burst frequency, increased linearly (Box 1) with the number of chambers included in the composite.

Reaction chamber volume was also increased by fabricating larger (5 and 10 μm diameter) individual chambers, allowing one individual expression resource pool to be shared by all of the genes. These larger chambers had proportionally more plasmids and resources, and once again the final protein abundance scaled linearly with volume (Figure 3a inset). Yet, in striking contrast to the composite 2 μm chambers, the CV^2 values of these shared resource chambers (large filled symbols in Figure 3a) were insensitive to abundance variation driven by changes in chamber volume (Figure 3a solid line; greater than a factor 25 change in abundance with less than a factor 3 change in CV^2). Notably, a composite of six individual 2 μm chambers, which is nearly equal in volume and final protein abundance to a single 5 μm chamber, produced a CV^2 approximately a factor of 5 lower than single 5 μm chambers (red box Figure 3a). This strikingly different noise behavior is not only apparent in the time histories of the expression experiments but also is seen in the distribution of final protein abundances seen across the populations of individual and composite reaction chambers (Figure 3b).

To confirm that this flat CV^2 trend across volumes was not unique to PDMS chambers, perhaps due to surface charge or molecular adsorption or absorption, we encapsulated PURE cell-free reactions expressing EGFP in more biologically similar

DOI: 10.1021/acssynbio.6b00189
ACS Synth. Biol. XXXX, XXX, XXX−XXX

Box 1

In bursty protein synthesis[37]

$$\langle P \rangle = \frac{B f_B}{\gamma_P}$$

$$CV^2 \approx \frac{\gamma_P}{f_B}$$

where $\langle P \rangle$ is the amount of protein produced and γ_P is the protein decay rate. The term f_B is often called the burst frequency, and it is a measure of how often a burst occurs. In the case of a single bursty gene, f_B is simply a frequency (Figure 1c) and is the inverse of the time period between adjacent burst events. If there are multiple copies of a gene, f_B is the average number of these genes that are active at any given time. B is the size of an expression burst, i.e., the average number of protein molecules produced in one expression burst.

Although protein abundance may be changed by either burst size or burst frequency, CV^2 is sensitive only to changes in burst frequency. As a result, CV^2 vs protein abundance plots reveal if abundance changes are driven primarily by changes in burst size or in burst frequency (see the graphic below). In the cell-free experiments reported here, systematic protein abundance changes were induced by changes in reaction chamber volume (i.e., by changes in the number of copies of the gene and the associated expression resources). Changes in protein abundance that induced little or no changes in CV^2 were indicative of changes in burst size with little or no change in burst frequency (figure below). In contrast, changes in protein abundance where CV^2 varied inversely with protein abundance were indicative of changes in burst frequency with little or no change in burst size (see the graphic below).

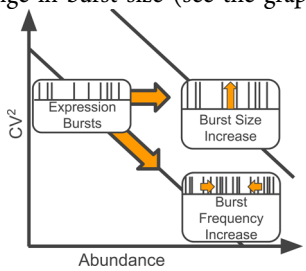

POPC water-in-water vesicles (Methods) and imaged them with confocal microscopy (Figure 2c). Vesicles ranged from about 4−19 μm in diameter (~65−3500 fL). Just as in the PDMS chambers, abundance scaled linearly with volume (Figure 3c inset), and CV^2 was only modestly sensitive to abundance changes across the range of volumes (e.g., fluorescent abundance increased by 3 orders of magnitude while CV^2 decreased by only 1 order of magnitude; solid line in Figure 3c).

While insensitive to systematic changes in protein abundance driven by changes in the reaction volume, CV^2 was hypersensitive to random fluctuations in protein abundance across a population of same-sized reaction chambers. Final protein abundance across the population of individual 2 μm chambers varied less than 1 order of magnitude, from 10^4 to 8×10^4 AU, but CV^2 varied more than an order of magnitude, from 10^{-2} to 3×10^{-4}. Similar behavior was observed across populations of 5 and 10 μm chambers as well (Figure 3d).

DISCUSSION

The most important implication of the results is that resource sharing and expression bursting are intimately linked. Sums of small discrete pools of resources achieved much lower expression noise than large shared pools, even with a constant ratio between DNA and expression resources (Figure 3a). These results lead to the inference that expression occurring in the large shared resource pool environments displays larger bursts (Box 1) than equal volume sums of discrete resource pools. The intriguing result is that instead of frequently consuming a small fraction of the available resources, individual genes are more apt to infrequently consume a large fraction of total resources. In a large shared volume, when both the pool of resources and the number of genes increased proportionally, the increased resources were drawn into making bursts larger (Figure 1c, right), not more frequent (Figure 1c, left). It seems that, given additional resources, expression bursts are more readily made bigger rather than made more often.

We investigated expression in the reaction chambers using a random telegraph[48,49] model of transcription from a group of genes competing for a shared population of translational resources (modeled here just as ribosomes; Figure 4a). In this model, genes switched between an OFF state with no transcription and an ON state where they produce uniquely identifiable mRNA molecules. Ribosomes diffused between a global pool and being bound to mRNA. Once bound to mRNA molecules, the ribosomes were less likely to rerandomize by diffusion back into the global pool, i e., $k_b \gg k_r$. To correspond with the experiments, we performed Gillespie simulations of this model and measured the CV^2 of the resulting protein population using exactly the same algorithms used for the experimental data (Methods). Small reaction chambers were modeled with a small number of genes drawing from a small pool of ribosomes, whereas larger reaction chambers were modeled as larger numbers of genes drawing from a proportionally larger pool of ribosomes. In agreement with the experimental data, larger reaction chambers led to a proportional increase in protein abundance, yet the CV^2 of this population remained flat (Figure 4b). The invariance of the CV^2 to protein abundance indicated that burst size, not frequency, was responsible for increasing protein abundance (Box 1).

Interestingly, examination of the different simulations showed that regardless of reaction chamber size a similar number of genes, those that burst ON early, captured a disproportionate percentage of the available translational resources. Conversely, genes that turned ON late captured very few translational resources. The net result was that in both small and large reaction chambers just a few mRNA dominated protein synthesis (Figure 4c). The dominant mRNA molecules in the bigger reaction chambers drew from a much larger pool of available translational resources, so in effect each of these mRNA molecules experienced larger translational bursts than dominant mRNA molecules in the smaller reactions. This model predicts that the larger protein populations found in larger reaction chambers resulted from the translational amplification of burst sizes, not the initiation of more bursts. In this model, larger chambers did indeed produce proportionally larger mRNA populations (Figure 4c inset), yet much of this mRNA was translationally inactive because earlier produced mRNA molecules had already sequestered translational resources (Figure 4d).

Although the model predicts that CV^2 is insensitive to abundance changes driven by volume increases, it predicts

DOI: 10.1021/acssynbio.6b00189
ACS Synth. Biol. XXXX, XXX, XXX−XXX

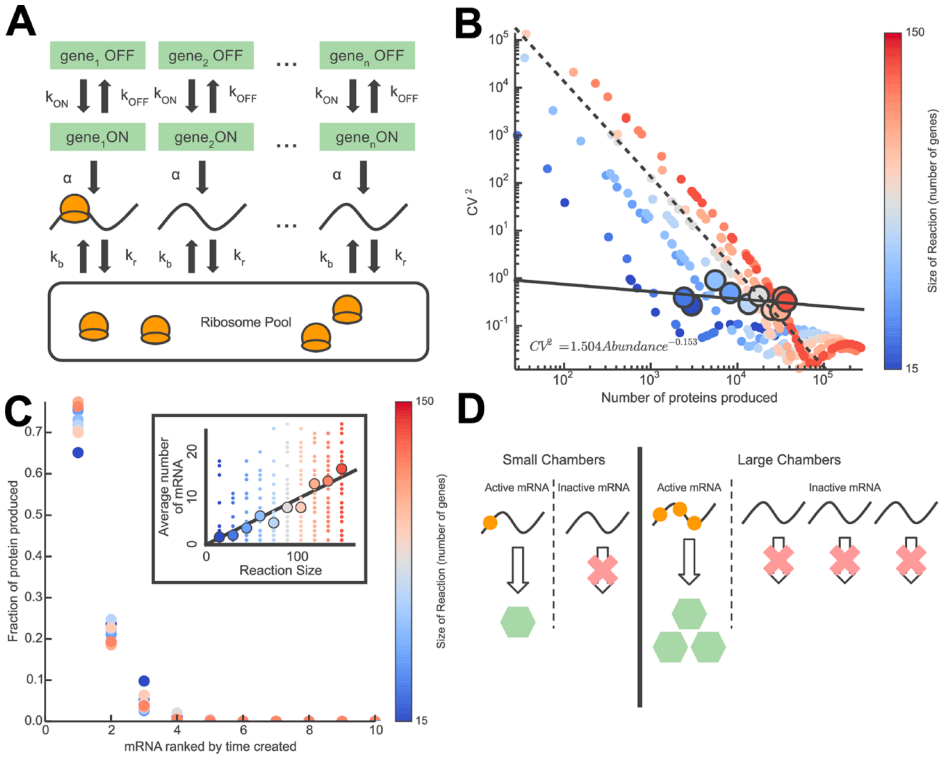

Figure 4. Model of the effects of resource pool size on expression bursting. (a) *In silico* model of resource sharing includes a resource pool of a limited number of reusable molecules, e.g., ribosomes, that associate with one of n genes (rate constant k_b) and return to the resource pool with rate constant k_r. The number of resources is proportional to the number of genes in each reaction. Genes burst ON and OFF at rates k_{ON} and k_{OFF}, respectively. Molecules of mRNA are created at rate α only in the ON state. (b) CV^2 vs protein abundance from the model described in (a). Colors represent the size of the reaction from 15 to 150 genes. Large points are means of multiple runs of the same reaction size. The solid line is a power law fit to all mean data points, and the dashed line is of the form a/abundance^2, where a is selected so that the line passes through the mean of a 105 gene reaction. As in the experimental chambers and vesicle data, CV^2 from this model is relatively insensitive to increases in abundance driven by changes in reaction sizes, but it is highly sensitive to increases in abundance that occur within a single reaction size. (c) mRNA molecules are ranked in the order of the time they were created. The y-axis shows the fraction of the total protein translated from each mRNA molecule. Points are colored by the reaction size (small reaction sizes are more blue, larger ones are more red). mRNA molecules made early, regardless of the reaction size, collected a disproportionate amount of resources and made a disproportionate amount of the total protein. The inset shows that mRNA abundance scales linearly with reaction size. (d) Schematic showing large reactions produced proportionally more mRNA molecules than small reactions, but most of this mRNA was inactive.

hypersensitivity (CV^2 α 1/abundnace^2; dashed line Figure 4b) to abundance variations that occur across chambers with the same volume. Examination of the simulation results showed that this strong relationship between CV^2 and abundance arose from the natural variability in the number of genes that initiated transcription early enough to effectively compete for ribosomes. Some runs of the simulation naturally showed a larger than average number of early turn-on genes, so these simulation trials exhibited a larger than average burst frequency. However, in these trials, a fixed population of ribosomes was distributed across this larger number of bursts, resulting in a reduction in the burst size. The prediction is a distribution of expression burst patterns across an ensemble of same-sized chambers where higher burst frequency is correlated with lower burst size (Supporting Information Figure 6). The net result is a distribution of final protein abundances and a CV^2 that declines sharply as protein abundance increases. In good agreement with this model prediction, CV^2 is highly sensitive to abundances changes across ensembles of same-sized PDMS chambers and POPC vesicles, and ensembles are well-fit by CV^2 α 1/abundance^2 (dashed lines in Figure 3c,d and Supporting Information Figure 7).

The results presented here suggest that expression bursts are self-reinforcing and that available translational resources are readily drawn into active transcriptional regions. This leads to the intriguing idea that, at least within prokaryotic cells, large translational bursts may be the direct result of large transcriptional bursts (Figure 5a). Recent work has shown that in *E. coli* large mRNA populations are strongly correlated with large transcriptional burst sizes[8] and that large protein populations are strongly correlated with larger translational burst sizes.[41] Taken together, these data demonstrate a strong correlation between transcriptional (B) and translational (b) burst sizes, with translational burst size increasing sharply ($b = 0.25 \times B^{4.77}$) with increased transcriptional burst size (Figure 5b). Although these data do not prove causation, this correlation does suggest strong cooperativity between the transcriptional and translational components of expression bursting. While the results presented here highlight the idea of transcriptional events controlling translational burst size, it is possible that there is mutual feedback, i.e., that a large transcriptional burst encourages a large translational burst, which in turn encourages an increase of the transcriptional burst size. Such mutual feedback would likely involve spatial effects such as beneficially crowding RNAP[50] or other crowding-enhanced localization of the ~100 components necessary for expression.[51]

Although it is well-known that expression bursting is a ubiquitous phenomenon, little is known about the possible benefits

DOI: 10.1021/acssynbio.6b00189
ACS Synth. Biol. XXXX, XXX, XXX−XXX

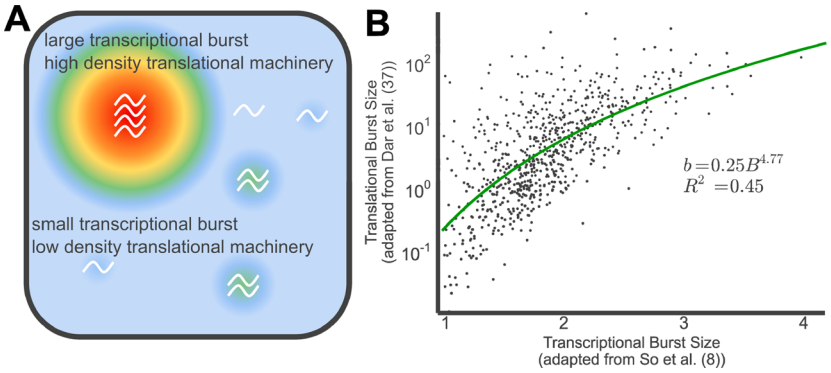

Figure 5. Correlation between transcriptional and translational burst sizes in *E. coli*. (a) Schematic of a large transcriptional burst sequestering a disproportionate amount of resources (heat map) leading to a large translational burst. (b) *E. coli* translational (adapted from ref 37) vs transcriptional (adapted from ref 8) burst sizes. Each data point is for an individual *E. coli* gene. The solid line is a power law fit as given by the equation in the graph.

of bursting. However, organism-scale gene expression presents a classic problem of optimizing the utility of limited shared resources. As the results presented here illustrate, expression bursting and resource sharing may be intimately linked phenomena. Expression bursting constrains a gene to draw heavily from the common resource pool over limited periods, yet it draws no resources the majority of the time. This pattern of resource sharing is reminiscent of packet mode communication,[52] which allows the capacity of a shared network to be efficiently divided across a variable number of messages. Although expression bursting is noisier than constitutive expression, it is certainly conceivable that it provides efficiency in the allocation of limited shared resources. Part of this efficiency may arise from the propensity—illustrated by the results presented here—to extend existing bursts instead of initiating new bursts. The initiation of new bursts requires the nucleation and assembly of expression machinery, while in contrast the extension of a burst leverages resources already in place. This preference for resource sharing through burst size, not burst frequency, modulation may explain recent results and analyses that have noticed burst frequency saturation in many cell types.[6,41,53] Indeed, other recent results have shown increased burst sizes in response to increased cell volume[54] or increased crowding in vesicles.[55] The picture that is emerging across multiple studies is one where protein abundance changes are preferentially mediated by modulation of burst size, not burst frequency. The results reported here clarify this picture by showing that expression resources are more readily pulled into existing bursts instead of going into the nucleation of more frequent bursts. Furthermore, these results suggest the intriguing idea that bursting is not just an artifact but instead may play a critical role in the optimal use of limited shared resources.

METHODS

Device Fabrication. A detailed description of device design and fabrication can be found elsewhere;[37,56] briefly, clean silicon wafers were coated in SU-8 photoresist. These were exposed to two patterns: one for the control valve and one for the channel. The patterns were developed, and extra SU-8 was washed off with isopropanol. The masters were silanized with trimethylchlorosilane. PDMS base and curing agent were thoroughly mixed at 20:1 and 5:1 ratios for the membrane and control valve, respectively, and degassed under vacuum. The membrane PDMS was spin-coated at 1000 rpm for 1 min over the control valve master. The channel PDMS was poured on the channel master, and both masters were partially cured at 80 °C. Channel masters were cut out, the control valve inlet hole was punched, and the channel master was aligned and bonded to the control valve. Aligned devices were baked for 2 h at 80 °C. Devices were cut out, inlet and outlet holes were punched, and the devices were plasma bonded to No. 0 coverslips.

Experimental Procedure (Chambers). A detailed description of the experimental procedure can be found in ref 37; briefly, devices were boiled in DI water for 1 h to hydrate the PDMS. Cell-free kits were mixed according to the manufacturer's instructions (Promega S30 T7 high-yield protein expression system). One 25 μL reaction was prepared with 500 ng of pet3a T7 EGFP plasmid, 10 μL of S30 premix, and 9 μL of T7 S30 extract and was filled to 25 μL with nuclease-free water. Reagents were mixed just before the experiment, and time was recorded when reagents were mixed. The reaction was then loaded into the hydrated device with <10 psi of low-grade nitrogen. The control valve was then pressurized with ∼20 psi of low-grade nitrogen. This sealed the individual chambers. The time between mixing reagents and sealing the chambers was about 4 min. The device was then placed on a Nikon Instruments Eclipse TE 300 inverted microscope and imaged through a Nikon N.A. 1.4, 100× oil objective with a Roper Scientific CoolSNAP-HQ CCD. Metamorph (Universal Imaging Corp., version 7.8.3.0) was used to capture images.

Experimental Procedure (Vesicles). Vesicle preparation was adapted from ref 57; briefly, an inner and outer solution were prepared. The inner solution contained 1 μL of Alexa 647 (15 ng of Alexa 647 transferin dissolved in 3 mL of water), 10 μL of PURE Solution A, 7.5 μL of PURE Solution B, 400 ng of pet3a T7 EGFP plasmid, 0.125 μL of RNAsin (40 U/μL), and 5 μL of sucrose (1 M) and was filled to 30 μL with nuclease-free water. The outer solution contained 3.6 μL of amino acid mix (50 mM), 4.9 μL of ATP (460 mM), 3.0 μL of GTP (500 mM), 1.5 μL of CTP (500 mM), 1.5 μL of UTP (500 mM), 3.6 μL of spermidine (250 mM), 7.5 μL of creatine phosphate (1 M), 9 μL of DTT (100 mM), 1.5 μL of folinic acid (4 mg/mL), 168 μL of potassium glutamate (1 M), 22.6 μL of magnesium acetate (0.5 M), 60 μL of HEPES (1 M), and 120 μL of glucose (1 M) and was filled to 600 μL with water. POPC (11.3 mg) was dissolved in 113 μL of chloroform. Of this mix, 30 μL was combined with 330 μL of paraffin oil and heated at 80 °C for 30 min. The POPC/paraffin oil mix was removed from heat, and the inner solution was added.

DOI: 10.1021/acssynbio.6b00189
ACS Synth. Biol. XXXX, XXX, XXX−XXX

The mixture was vortexed for 30 s to create an emulsion. The emulsion was layered on top of the outer solution and centrifuged for 20 min at 13 200 g and 4 °C. The bottom 100 μL of outer solution and vesicle pellet was pipetted onto a Petri dish with a No. 1.5 coverslip bottom.

Resource Sharing Model. The resource sharing model was simulated using a Gillespie algorithm. The model consisted of a fixed pool of available ribosomes equal to 100 times the number of genes in the simulation (roughly corresponding to the number of ribosomes per plasmid in the cell-free reactions[51]). Genes stochastically bursted[8] ON and OFF with rates k_{ON} and k_{OFF} (0.0002 min^{-1}, 0.2 min^{-1}), respectively. While in the ON state, genes produced mRNA at rate α (1 min^{-1}). Ribosomes bound mRNA molecules with rate constant k_b (1 min^{-1}) and returned to the pool with rate constant k_r (0.0001 min^{-1}). The rate of protein production per bound ribosome, k_p, decayed with time, $e^{-0.05t}$, to capture the decay in synthesis capacity observed in cell-free reactions.[36,44]

Data Acquisition and Analysis. *Image Processing (Chambers).* Metamorph (Universal Imaging Corp., version 7.8.3.0) recorded images as .tif files. These files were read with Fiji (Fiji is just ImageJ, version 2.0.0-rc-14/1.49g). Images were captured by hand, so the chambers moved frame-to-frame. Images were aligned with the Fiji plugin StackReg. To make region-of-interest (ROI) placement easier, aligned stacks were averaged. ROI centers were located using an automated Hough circle finding algorithm. The averaged image was used to determine the center of the individual reaction chambers for the 5 and 10 μm chambers. For the 2 μm chambers, the exterior edges of the dark chamber walls were estimated, and the center was estimated by finding the highest local intensity value within a 30 pixel radius of the center of the found circle. Centers found were fed into a Matlab script, which summed the intensity values of all pixels within a given radius of the center. ROI radii for every chamber in each of the three defined chamber sizes, 10, 5, and 2 μm, were 23, 10, and 5 pixels, respectively.

Image Processing (Vesicles). The vesicles settled to the coverslip and were imaged at 26 °C for 3 h with a 63× confocal oil objective on a Zeiss LSM710 confocal scanning microscope. Frames were recorded every 3 min as a *z*-stack of between 25 and 35 slices that were 1 μm thick each. The *z*-stack time series files were loaded into Fiji. Vesicles were found with the plugin TrackMate. Spots were filtered with an estimated diameter of 10 μm, a signal-to-noise ratio >0, and a contrast >0. Trackmate stitched together found vesicles into traces. Traces were filtered with duration >90 min, no gaps, jumps between frames <5 μm, and a total track displacement <11.9 μm. Traces that remained, and existed for the entire third hour of the experiment, were analyzed by the same noise extraction method described below.

Noise Extraction. The method for noise extraction was adapted from ref 46, where it is explained in more detail. Experiments were sorted by chamber size (indexed by s = 2, 5, and 10) and day of experiment (indexed as d = 1, 2, 3, 4, and 5). General trends of fluorescence signals ($A_{s,d}$) were calculated as

$$A_{s,d}(kT) = \frac{\sum_{m=1}^{M} I_{m,s,d}(kT)}{M}$$

where T is the time interval between measurements of fluorescent intensity and k = 0, 1, 2, ... K is the sample number; m = 1, ..., M represents each of the M individual chambers of a given size imaged during a given day; and $I_{m,s,d}(kT)$ is the time-dependent fluorescent intensity of an individual reaction chamber as measured by the procedure above

Noise ($N_{m,s,d}(kT)$) was defined as

$$N_{m,s,d}(kT) \equiv I_{m,s,d}(kT) - g_{m,s,d} \cdot A_{s,d}(kT)$$

where $g_{m,s,d}$ is a gain factor that describes the extent to which the general trend coupled into each individual noise trajectory. The $g_{m,s,d}$ values were selected to minimize the cross-correlation[45] between $N_{m,s,d}(kT)$ and $A_{s,d}(kT)$. CV^2 was calculated as

$$CV^2_{m,s,d} = \frac{\sigma^2_{N_{m,s,d}}}{I^2_{m,s,d}(\text{final})}$$

where $I_{m,s,d}$(final) is the final fluorescence level measured at the end point of the experiments.

Chamber Combination Analysis. Two-hundred composite noise traces were created by randomly combining without replacement between two and six of the 45 individual 2 μm chambers imaged in the experiments. Composite chambers had no more than three individual 2 μm chambers in common with any other composite chamber. The fluorescent abundances of the composite chambers were found by summing the abundances of each individual chamber in the composite chamber. The variances of the composite chambers were found using the sums of the extracted noise of each individual chamber in the composite. The CV^2 of each composite chamber was defined as the composite variance divided by the composite abundance squared. The volume of composite chambers was found as the sum of the individual chambers in the composite.

Calculating mRNA Contributions. The reaction size of the model was varied by changing the number of genes in the system from 15 to 150 genes in increments of 15 (indexed by g = 15, 30, 45, ..., 150). Fifty trajectories (indexed as c = 1, 2, 3, ..., 50) were simulated for each reaction size. mRNA molecules were created and indexed by l = 1, 2, 3, ..., L in the order in which they were created (i.e., the first mRNA made was ranked l = 1). The number of ribosomes bound to an mRNA molecule was $R_{c,g,l,k}$, where k was the sample number (k = 0, 1, 2, ..., K). The protein production rate decayed exponentially, $k_p = e^{-0.05(kT)}$, over the duration of the experiment. The decay modeled the loss of expression capacity observed in cell-free reactions.[36,44] The total number of protein produced, $P_{c,g,l}$, from each mRNA at each sample number was calculated by summing the product of the number of bound ribosomes and the protein production rate for each minute of the simulated experiment.

$$P_{c,g,l} = \sum_{k=0}^{K} R_{c,g,l,k}\, e^{-0.05(kT)}$$

where T is the interval between samples. The average number of protein produced by mRNA molecules of each rank was calculated as

$$P_{g,l} = \frac{1}{C} \sum_{c=1}^{C} P_{c,g,l}$$

The average protein population associated with an individual mRNA molecule was normalized by the total amount of protein produced and was calculated as

$$P_{\text{NORM}g,l} = \frac{P_{g,l}}{\sum_{l=1}^{L} P_{g,l}}$$

DOI: 10.1021/acssynbio.6b00189
ACS Synth. Biol. XXXX, XXX, XXX−XXX

This normalization, $P_{NORMg,b}$ when plotted against mRNA rank, j, illustrated the relative influence of mRNA rank on the final protein population.

■ ASSOCIATED CONTENT

Supporting Information

The Supporting Information is available free of charge on the ACS Publications website at DOI: 10.1021/acssynbio.6b00189.

Additional experimental and computational results (PDF)

■ AUTHOR INFORMATION

Corresponding Author

*E-mail: SimpsonML1@ornl.gov.

Notes

The authors declare no competing financial interest.

■ ACKNOWLEDGMENTS

This research was conducted at the Center for Nanophase Materials Sciences, which is a DOE Office of Science User Facility. P.M.C., S.E.N., and C.W.C. also acknowledge Graduate Fellowships from the Bredesen Center for Interdisciplinary Research and Graduate Education, University of Tennessee, Knoxville. M.L.S. also acknowledges support from the University of Tennessee/Oak Ridge National Laboratory Joint Institute for Biological Sciences. B.S.R. also acknowledges support from a Merck Postdoctoral Fellowship at the Rockefeller University.

■ REFERENCES

(1) Hensel, Z., Feng, H., Han, B., Hatem, C., Wang, J., and Xiao, J. (2012) Stochastic expression dynamics of a transcription factor revealed by single-molecule noise analysis. *Nat. Struct. Mol. Biol. 19*, 797−802.

(2) Levine, J. H., Lin, Y., and Elowitz, M. B. (2013) Functional roles of pulsing in genetic circuits. *Science 342*, 1193−1200.

(3) Blake, W. J., Kaern, M., Cantor, C. R., and Collins, J. J. (2003) Noise in eukaryotic gene expression. *Nature 422*, 633−637.

(4) Taniguchi, Y., Choi, P. J., Li, G.-W., Chen, H., Babu, M., Hearn, J., Emili, A., and Xie, X. S. (2010) Quantifying E. coli proteome and transcriptome with single-molecule sensitivity in single cells. *Science 329*, 533−538.

(5) Carey, L. B., Van Dijk, D., Sloot, P. M. A., Kaandorp, J. A., and Segal, E. (2013) Promoter sequence determines the relationship between expression level and noise. *PLoS Biol. 11*, e1001528.

(6) Dar, R. D., Razooky, B. S., Singh, A., Trimeloni, T. V., McCollum, J. M., Cox, C. D., Simpson, M. L., and Weinberger, L. S. (2012) Transcriptional burst frequency and burst size are equally modulated across the human genome. *Proc. Natl. Acad. Sci. U. S. A. 109*, 17454−17459.

(7) Skupsky, R., Burnett, J. C., Foley, J. E., Schaffer, D. V., and Arkin, A. P. (2010) HIV promoter integration site primarily modulates transcriptional burst size rather than frequency. *PLoS Comput. Biol. 6*, e1000952.

(8) So, L., Ghosh, A., Zong, C., Sepúlveda, L. A., Segev, R., and Golding, I. (2011) General properties of transcriptional time series in Escherichia coli. *Nat. Genet. 43*, 554−560.

(9) Kaern, M., Elston, T. C., Blake, W. J., and Collins, J. J. (2005) Stochasticity in gene expression: from theories to phenotypes. *Nat. Rev. Genet. 6*, 451−464.

(10) Ceroni, F., Algar, R., Stan, G.-B., and Ellis, T. (2015) Quantifying cellular capacity identifies gene expression designs with reduced burden. *Nat. Methods 12*, 415−418.

(11) Gyorgy, A., and Del Vecchio, D. (2014) *Limitations and trade-offs in gene expression due to competition for shared cellular resources*, IEEE 53rd Annual Conference on Decision and Control (CDC), pp 5431−5436.

(12) Guantes, R., Díaz-Colunga, J., and Iborra, F. J. (2016) Mitochondria and the non-genetic origins of cell-to-cell variability: More is different. *BioEssays 38*, 64.

(13) De Vos, D., Bruggeman, F. J., Westerhoff, H. V., Bakker, B. M., et al. (2011) How molecular competition influences fluxes in gene expression networks. *PLoS One 6*, e28494−e28494.

(14) Siegal-Gaskins, D., Tuza, Z. A., Kim, J., Noireaux, V., and Murray, R. M. (2014) Gene circuit performance characterization and resource usage in a cell-free "breadboard. *ACS Synth. Biol. 3*, 416−425.

(15) Mather, W. H., Hasty, J., Tsimring, L. S., and Williams, R. J. (2013) Translational cross talk in gene networks. *Biophys. J. 104*, 2564−2572.

(16) Kepler, T. B., and Elston, T. C. (2001) Stochasticity in transcriptional regulation: origins, consequences, and mathematical representations. *Biophys. J. 81*, 3116−3136.

(17) Simpson, M. L., Cox, C. D., and Sayler, G. S. (2004) Frequency domain chemical Langevin analysis of stochasticity in gene transcriptional regulation. *J. Theor. Biol. 229*, 383−394.

(18) To, T.-L., and Maheshri, N. (2010) Noise can induce bimodality in positive transcriptional feedback loops without bistability. *Science 327*, 1142−1145.

(19) Sanchez, A., Garcia, H. G., Jones, D., Phillips, R., and Kondev, J. (2011) Effect of promoter architecture on the cell-to-cell variability in gene expression. *PLoS Comput. Biol. 7*, e1001100.

(20) Blake, W. J., Balázsi, G., Kohanski, M. A., Isaacs, F. J., Murphy, K. F., Kuang, Y., Cantor, C. R., Walt, D. R., and Collins, J. J. (2006) Phenotypic consequences of promoter-mediated transcriptional noise. *Mol. Cell 24*, 853−865.

(21) Raj, A., Peskin, C. S., Tranchina, D., Vargas, D. Y., and Tyagi, S. (2006) Stochastic mRNA synthesis in mammalian cells. *PLoS Biol. 4*, e309.

(22) Suter, D. M., Molina, N., Gatfield, D., Schneider, K., Schibler, U., and Naef, F. (2011) Mammalian genes are transcribed with widely different bursting kinetics. *Science 332*, 472−474.

(23) Raser, J. M., and O'Shea, E. K. (2004) Control of stochasticity in eukaryotic gene expression. *Science 304*, 1811−1814.

(24) Chong, S., Chen, C., Ge, H., and Xie, X. S. (2014) Mechanism of transcriptional bursting in bacteria. *Cell 158*, 314−326.

(25) Golding, I., Paulsson, J., Zawilski, S. M., and Cox, E. C. (2005) Real-time kinetics of gene activity in individual bacteria. *Cell 123*, 1025−1036.

(26) Zenklusen, D., Larson, D. R., and Singer, R. H. (2008) Single-RNA counting reveals alternative modes of gene expression in yeast. *Nat. Struct. Mol. Biol. 15*, 1263−1271.

(27) Chubb, J. R., Trcek, T., Shenoy, S. M., and Singer, R. H. (2006) Transcriptional pulsing of a developmental gene. *Curr. Biol. 16*, 1018−1025.

(28) Yu, J., Xiao, J., Ren, X., Lao, K., and Xie, X. S. (2006) Probing gene expression in live cells, one protein molecule at a time. *Science 311*, 1600−1603.

(29) Dar, R. D., Karig, D. K., Cooke, J. F., Cox, C. D., and Simpson, M. L. (2010) Distribution and regulation of stochasticity and plasticity in Saccharomyces cerevisiae. *Chaos 20*, 037106.

(30) Bar-Even, A., Paulsson, J., Maheshri, N., Carmi, M., O'Shea, E., Pilpel, Y., and Barkai, N. (2006) Noise in protein expression scales with natural protein abundance. *Nat. Genet. 38*, 636−643.

(31) Retterer, S. T., Siuti, P., Choi, C.-K., Thomas, D. K., and Doktycz, M. J. (2010) Development and fabrication of nanoporous silicon-based bioreactors within a microfluidic chip. *Lab Chip 10*, 1174−1181.

(32) Siuti, P., Retterer, S. T., and Doktycz, M. J. (2011) Continuous protein production in nanoporous, picolitre volume containers. *Lab Chip 11*, 3523−3529.

(33) Siuti, P., Retterer, S. T., Choi, C.-K., and Doktycz, M. J. (2012) Enzyme reactions in nanoporous, picoliter volume containers. *Anal. Chem. 84*, 1092−1097.

(34) Jewett, M. C., and Swartz, J. R. (2004) Mimicking the Escherichia coli cytoplasmic environment activates long-lived and efficient cell-free protein synthesis. *Biotechnol. Bioeng. 86*, 19−26.

DOI: 10.1021/acssynbio.6b00189
ACS Synth. Biol. XXXX, XXX, XXX−XXX

(35) Jewett, M. C., Calhoun, K. A., Voloshin, A., Wuu, J. J., and Swartz, J. R. (2008) An integrated cell-free metabolic platform for protein production and synthetic biology. *Mol. Syst. Biol. 4*, 220.
(36) Karig, D. K., Jung, S.-Y., Srijanto, B., Collier, C. P., and Simpson, M. L. (2013) Probing cell-free gene expression noise in femtoliter volumes. *ACS Synth. Biol. 2*, 497−505.
(37) Norred, S. E., Caveney, P. M., Retterer, S. T., Boreyko, J. B., Fowlkes, J. D., Collier, C. P., and Simpson, M. L. (2015) Sealable Femtoliter Chamber Arrays for Cell-free Biology. *J. Visualized Exp.*, e52616.
(38) Ozbudak, E. M., Thattai, M., Kurtser, I., Grossman, A. D., and van Oudenaarden, A. (2002) Regulation of noise in the expression of a single gene. *Nat. Genet. 31*, 69−73.
(39) Munsky, B., Neuert, G., and van Oudenaarden, A. (2012) Using gene expression noise to understand gene regulation. *Science 336*, 183−187.
(40) Dey, S. S., Foley, J. E., Limsirichai, P., Schaffer, D. V., and Arkin, A. P. (2015) Orthogonal control of expression mean and variance by epigenetic features at different genomic loci. *Mol. Syst. Biol. 11*, 806.
(41) Dar, R. D., Razooky, B. S., Weinberger, L. S., Cox, C. D., and Simpson, M. L. (2015) The Low Noise Limit in Gene Expression. *PLoS One 10*, e0140969.
(42) Nomura, S. M., Tsumoto, K., Hamada, T., Akiyoshi, K., Nakatani, Y., and Yoshikawa, K. (2003) Gene expression within cell-sized lipid vesicles. *ChemBioChem 4*, 1172−1175.
(43) Kato, A., Yanagisawa, M., Sato, Y. T., Fujiwara, K., and Yoshikawa, K. (2012) Cell-sized confinement in microspheres accelerates the reaction of gene expression. *Sci. Rep. 2*, 283.
(44) Sun, Z. Z., Hayes, C. A., Shin, J., Caschera, F., Murray, R. M., and Noireaux, V. (2013) Protocols for implementing an Escherichia coli based TX-TL cell-free expression system for synthetic biology. *J. Visualized Exp.*, e50762.
(45) Austin, D. W., Allen, M. S., McCollum, J. M., Dar, R. D., Wilgus, J. R., Sayler, G. S., Samatova, N. F., Cox, C. D., and Simpson, M. L. (2006) Gene network shaping of inherent noise spectra. *Nature 439*, 608−611.
(46) Weinberger, L. S., Dar, R. D., and Simpson, M. L. (2008) Transient-mediated fate determination in a transcriptional circuit of HIV. *Nat. Genet. 40*, 466−470.
(47) Newman, J. R., Ghaemmaghami, S., Ihmels, J., Breslow, D. K., Noble, M., DeRisi, J. L., and Weissman, J. S. (2006) Single-cell proteomic analysis of S. cerevisiae reveals the architecture of biological noise. *Nature 441*, 840−846.
(48) Peccoud, J., and Ycart, B. (1995) Markovian modeling of gene-product synthesis. *Theor. Popul. Biol. 48*, 222−234.
(49) Paulsson, J. (2004) Summing up the noise in gene networks. *Nature 427*, 415−418.
(50) Ge, X., Luo, D., and Xu, J. (2011) Cell-free protein expression under macromolecular crowding conditions. *PLoS One 6*, e28707.
(51) Shimizu, Y., Inoue, A., Tomari, Y., Suzuki, T., Yokogawa, T., Nishikawa, K., and Ueda, T. (2001) Cell-free translation reconstituted with purified components. *Nat. Biotechnol. 19*, 751−755.
(52) Chandra, K. (2011) Statistical Time Division Multiplexing. *Handbook of Computer Networks 1*, 579−590.
(53) Sanchez, A., and Golding, I. (2013) Genetic determinants and cellular constraints in noisy gene expression. *Science 342*, 1188−1193.
(54) Padovan-Merhar, O., Nair, G. P., Biaesch, A. G., Mayer, A., Scarfone, S., Foley, S. W., Wu, A. R., Churchman, L. S., Singh, A., and Raj, A. (2015) Single Mammalian Cells Compensate for Differences in Cellular Volume and DNA Copy Number through Independent Global Transcriptional Mechanisms. *Mol. Cell 58*, 339−352.
(55) Hansen, M. M., Meijer, L. H., Spruijt, E., Maas, R. J., Rosquelles, M. V., Groen, J., Heus, H. A., and Huck, W. T. (2015) Macromolecular crowding creates heterogeneous environments of gene expression in picolitre droplets. *Nat. Nanotechnol. 11*, 191−197.
(56) Fowlkes, J. D., and Collier, C. P. (2013) Single-molecule mobility in confined and crowded femtolitre chambers. *Lab Chip 13*, 877−885.
(57) Nishimura, K., Tsuru, S., Suzuki, H., and Yomo, T. (2015) Stochasticity in gene expression in a cell-sized compartment. *ACS Synth. Biol. 4*, 566−576.

DOI: 10.1021/acssynbio.6b00189
ACS Synth. Biol. XXXX, XXX, XXX−XXX